Removal of trace mercury (II) from aqueous solution by *in situ* MnO_x combined with poly-aluminum chloride

Xixin Lu, Xiaoliu Huangfu, Xiang Zhang, Yaan Wang and Jun Ma

ABSTRACT

Removal of trace mercury from aqueous solution by Mn (hydr)oxides formed *in situ* during coagulation with poly-aluminum chloride (PAC) (*in situ* MnO_x combined with PAC) was investigated. The efficiency of trace mercury removal was evaluated under the experimental conditions of reaction time, Mn dosage, pH, and temperature. In addition, the ionic strength and the initial mercury concentration were examined to evaluate trace mercury removal for different water qualities. The results clearly demonstrated that *in situ* MnO_x combined with PAC was effective for trace mercury removal from aqueous solution. A mercury removal ratio of 9.7 μg Hg/mg Mn was obtained at pH 3. Furthermore, at an initial mercury concentration of 30 μg/L and pH levels of both 3 and 5, a Mn dosage of 4 mg/L was able to lower the mercury concentration to meet the standards for drinking water quality at less than 1 μg/L. Analysis by Fourier transform infrared spectroscopy and X-ray photoelectron spectroscopy suggests that the hydroxyls on the surface of Mn (hydr)oxides are the active sites for adsorption of trace mercury from aqueous solution.

Key words | *in situ*, Mn (hydr)oxides, PAC, trace mercury

Xixin Lu
Xiaoliu Huangfu
Xiang Zhang
Yaan Wang
Jun Ma (corresponding author)
State Key Laboratory of Urban Water Resource and Environment,
School of Municipal and Environmental Engineering,
Harbin Institute of Technology,
Harbin 150090,
China
E-mail: *majun@hit.edu.cn*

INTRODUCTION

Mercury (Hg(II)) is regarded as one of the most harmful toxic metals in the environment (Zabihi *et al.* 2010). Many countries have suffered from mercury pollution, including Iraq, Brazil, Indonesia, the USA, and China (Jiang *et al.* 2006). Mercury can enter water supplies through industrial waste from various sources such as chloralkali, mining, and metallurgical processes (Weisener *et al.* 2005). As a result, mercury pollution of water, in particular, has created serious environmental problems (Brown *et al.* 1979). It is well known that mercury can be harmful to many forms of life, including humans, through bioaccumulation of the toxic metal (Sari & Tuzen 2009). Toxicological studies have indicated that some types of mercury damage the human body through the central nervous system (Sari & Tuzen 2009). Furthermore, even very low levels of mercury in drinking water may be dangerous for humans (Blue *et al.* 2008; Li *et al.* 2011). The US Environmental Protection Agency, the World Health Organization (WHO), and China have all recognized this serious health threat and have set standards for maximum mercury levels in drinking water at 2.0, 1.0, and 1.0 μg/L, respectively (Li *et al.* 2011). Therefore, it is clear that mercury pollution in drinking water needs to be controlled.

The conventional methods for mercury removal from water are biosorption (Wagner-Dobler *et al.* 2000; Inbaraj *et al.* 2009), adsorption (Jeon & Park 2005; Sumesh *et al.* 2011; Xu *et al.* 2011), ion exchange (Ratto *et al.* 2000; Anirudhan *et al.* 2008), and chemical precipitation (Brown *et al.* 1979; Skyllberg & Drott 2010). However, these methods are used primarily for the treatment of aqueous solutions that contain high mercury concentrations; they may not be effective for achieving the low levels of mercury that meet the standards for drinking water quality. Presently, there are only a few methods that can be applied for trace mercury removal from water (Blue *et al.* 2008). One such method is enhanced coagulation, which has many advantages such as lower cost, shorter hydraulic retention time, and lack of complicated treatment structures. Thus, enhanced

doi: 10.2166/wh.2014.156

coagulation has frequently been studied as the method of choice to remove water contaminants such as algae (Wu *et al.* 2011), arsenic (Song *et al.* 2006), organic matter (Yan *et al.* 2008), color (Jiang & Graham 1996), and phosphorus (Zhou *et al.* 2008). Certain types of enhanced coagulation have even been applied in water treatment plants (Yan *et al.* 2006; Guo *et al.* 2011).

There are several types of enhanced coagulation such as increasing coagulant dosage, change of pH, addition of coagulant aid, and optimization of process. An adsorption–flocculation process as an enhanced coagulation technology is used in our work. The enhanced coagulation resulting from the combination of *in situ*-formed manganese (hydr)oxides (Mn (hydr)oxides) with poly-aluminum chloride (PAC) is an adsorption–flocculation process. In an early study, manganese dioxide (MnO_2) produced from permanganate oxidation was shown to enhance flocculation and filtration of contaminants from water of both high and low turbidity (Ma *et al.* 1997). A more recent study showed that organic pollutants are adsorbed by MnO_2 formed *in situ*; in addition, atomic force microscope analysis indicated that MnO_2 formed *in situ* has smaller particle sizes, and consequently higher adsorption capacities than the aged MnO_2 (Zhang *et al.* 2008). These studies highlight the ability of *in situ* MnO_x to deal with pollutants. However, to date, the enhanced removal of mercury from drinking water by *in situ* MnO_x in combination with PAC coagulation has not yet been studied. In this adsorption–flocculation process, the *in situ* MnO_x transfers mercury to the solid phase. However, since *in situ* MnO_x particles are small, PAC is used as a flocculant to settle the Hg–Mn particles.

In this work, trace mercury removal efficiency of enhanced coagulation, or adsorption–flocculation, using *in situ* MnO_x combined with PAC was examined. Contaminated drinking water was simulated with trace mercury solutions, and the effect on water quality was investigated by varying pH and ionic strength. Optimum test conditions for trace mercury removal were determined as a function of reaction time, chemical dosage, pH, and temperature. Moreover, a possible mechanism of trace mercury removal was determined using Fourier transform infrared spectroscopy (FTIR) and X-ray photoelectron spectroscopy (XPS). Finally, water was obtained from a drinking water source, and trace mercury removal by *in situ* MnO_x combined with PAC was carried out.

MATERIALS AND METHODS

Materials

Reagents of analytical grade purity were used in these experiments except for nitric acid (HNO_3), which was of metal-oxide-semiconductor (MOS) grade purity. Mercuric nitrate ($Hg(NO_3)_2$) was obtained from Jiangyan Huanqiu Reagent Company (China). Other chemicals used were purchased from Sinopharm Chemical Reagent Co., Ltd, China.

Freshly distilled water was used for water solutions. The stock solution of mercury (1,000 mg Hg/L) was prepared by dissolving mercuric nitrate ($Hg(NO_3)_2$) in 2% HNO_3 solution and then diluting with water to achieve the desired concentrations in trace mercury solutions. The solutions of sodium thiosulfate ($Na_2S_2O_3$) and L-cysteine were prepared immediately prior to use. PAC was purchased from Sinopharm Chemical Reagent Co., Ltd, China. For the PAC solutions in this study, the ratio of active species in the stock solution was above 10% as Al_2O_3. PAC solutions were diluted with distilled water to get 20 g Al/L dilution for use. Reagents were stored tightly capped at 4 °C until needed.

Trace mercury solutions were prepared at various concentrations by diluting the stock mercury solution with freshly distilled water. The alkalinity and ionic strength of drinking water were simulated by addition of 0.001 mol/L sodium bicarbonate ($NaHCO_3$) and 0.01 mol/L sodium chloride (NaCl) to these mercury solutions.

In situ-formed Mn (hydr)oxides were formed by adding potassium permanganate ($KMnO_4$) and $Na_2S_2O_3$ at a molar ratio of 1.5 into trace mercury solutions needed for water treatment.

All glassware was cleaned by first soaking in HNO_3 solution (10–20%) for 24 hours and then rinsing three times with tap water, followed by distilled water. The mercury concentration of distilled water in the glassware was detected to ensure the glassware was clean, and all detection values were less than 0.1 μg/L (for Hg). After coagulation and rinsing, the experimental wastewater containing mercury was

collected and treated in the professional wastewater treatment plant to guard against mercury pollution.

Batch experiments

Standard jar tests were performed as with a conventional coagulation process. In the first step of the experimental procedure, *in situ* MnO_x was added into 1 L of trace mercury solution. The solution was stirred rapidly for 2 minutes at 150 rpm and then stirred slowly for 15 minutes at 40 rpm to facilitate mercury adsorption. PAC was then added, and the solution was stirred rapidly for 2 minutes and then slowly for 15 minutes during flocculation. Lastly, the solution was left sitting for 30 minutes to allow particles (flocs) to settle; the supernatant was removed and filtered prior to taking samples.

Each experiment was conducted in duplicate. The blank checks were performed to ensure that mercury was not found in the distilled water used in the samples, and all detection values were less than 0.1 μ/L (for Hg). The control experiment was designed to investigate the ability of *in situ* MnO_x, in which PAC was the coagulant used to remove mercury in the distilled water system, as PAC may affect mercury removal by *in situ* MnO_x in the adsorption process. In the jar tests, PAC was added to *in situ* MnO_x solutions to accelerate the aggregation and precipitate of *in situ* MnO_x. However, there was no obvious removal of mercury by PAC (figures not shown).

To determine optimum test conditions, the stirring time varied from 0 to 62 minutes, the Mn dosage was varied from 0 to 10 mg Mn/L, the PAC dosage was 5 mg Al/L, pH varied from 3.0 to 9.0, temperature was varied from 5 to 35 °C, and the ionic strength was varied from 0.001 to 0.1 mol/L. In the experimental process, when one of the factors was studied, other factors were kept constant. If not otherwise specified, the solution pH, Mn dosage, temperature, and initial concentration of mercury in the trace mercury solutions were 7.0 ± 0.1, 4 mg Mn/L, 25 °C, and 30 μg/L, respectively. The solution pH was kept constant by adding a series of concentrations of hydrochloric acid (HCl) and sodium hydroxide (NaOH).

Actual drinking water was collected from the Songhua River (Harbin, China) and used as a mercury-contaminated model by the addition of mercury. In these tests, the solution pH was not kept fixed. The quality parameters of mercury concentration, temperature, pH, turbidity, and total alkalinity for this drinking water were 0.02 μg/L, 24 ± 1 °C, 6.8–7.1, 5.2–6.2 nephelometric turbidity units (NTU), and 120–133 mg/L $CaCO_3$, respectively. The actual water was spiked to obtain the initial mercury concentration (30 μg/L) in the experiments.

Analytical methods

The supernatant was taken and filtered immediately through a cellulose acetate membrane of 0.22 μm pore size. The mercury concentration of contaminated water alone after filtration was tested, and the results showed that there was no change in the mercury concentration, indicating that the filters were clean. Then, the samples were acidified with HNO_3 (2%). Total mercury concentration was detected using an inductively coupled plasma mass spectrometry (ICP-MS) spectrometer (NexION 300 Q, PerkinElmer Inc.). Before every sample measurement, a solution prepared by dissolving L-cysteine in 2% HNO_3 (MOS) (1 mg/L L-cysteine solution) was used to rinse the tubes used for ICP-MS analysis. Error bars in figures represent the standard deviation of the mean.

FTIR and XPS analysis

The initial mercury concentration and Mn dosage were 500 μg/L and 20 mg Mn/L, respectively. The precipitates were collected, washed with distilled water, and then freeze–dried in vacuum before FTIR and XPS analysis. FTIR spectra were collected on a Spectrum One B spectrometer (PerkinElmer Inc.).

The XPS measurements were performed on a spectrometer (K–Alpha, Thermofisher Scientific Company) with 350 kcps sensitivity, using an AlKa source (2,000 eV). The vacuum chamber was 1.0×10^{-8} mbar in the analysis room. All spectra were measured in a 400 μm diameter analysis area. The high-resolution scans were recorded using fixed pass energy of 50 eV and a scanning step of 0.1 eV. The method of depth profiling was Ar erosion, using energy of 2,000 eV, area of 2 mm, and speed of 0.3 nm/s. A binging energy of 284.5 eV was used for C1s peak as an inner calibration standard.

RESULTS AND DISCUSSION

Effect of stirring time

Figure 1(a) shows that trace mercury removal was affected by stirring time. As stirring time was increased from 0 to 62 minutes, mercury removal increased from 0 to 93%. For an increase from 0 to 7 minutes of stirring time, mercury removal increased rapidly to 50%. This was followed by a slow increase of mercury removal to 93% in the stirring time range of 12–42 minutes. After 42 minutes, the removal ratio remained approximately constant. When they are first formed, the particles of *in situ* MnO_x have been shown to be very small and unregulated, with diameters varying from 20 to 100 nm (Zhang *et al.* 2008). Thus, *in situ* MnO_x particles have a greater surface area early on after formation (Zhang *et al.* 2008). At shorter time scales, the particles may have many active adsorption sites on their surfaces, leading to a rapid increase of mercury removal efficiency. However, as the processes of stirring and adsorption proceed, the particles of *in situ* MnO_x become larger (Zhang *et al.* 2008) and the surface active sites likely decrease, resulting in a slower mercury removal ratio.

Thus, *in situ* MnO_x may have lots of active adsorption sites on the surface, leading to a rapid increase of mercury removal ratio. As the processes of stirring and adsorption proceeded, the particles of *in situ* MnO_x became larger (Zhang *et al.* 2008) and the surface active sites decreased so that the mercury removal rate became slower.

Effect of Mn dosage

Mercury removal increased with increasing Mn dosage (Figure 1(b)). The mercury removal ratio was 10% when the Mn dosage was 2 mg/L. For the Mn dosage increase from 4 to 7 mg/L, the mercury removal ratio increased from 42 to 98%. The surface active sites on Mn may be much more abundant with increasing Mn dosage, resulting in increased mercury removal (Guan *et al.* 2009a, b). In these experiments, the initial mercury concentration was 30 μg/L, and a mercury concentration of less than 1 μg/L was achieved with an Mn dosage of 7 mg/L. In other

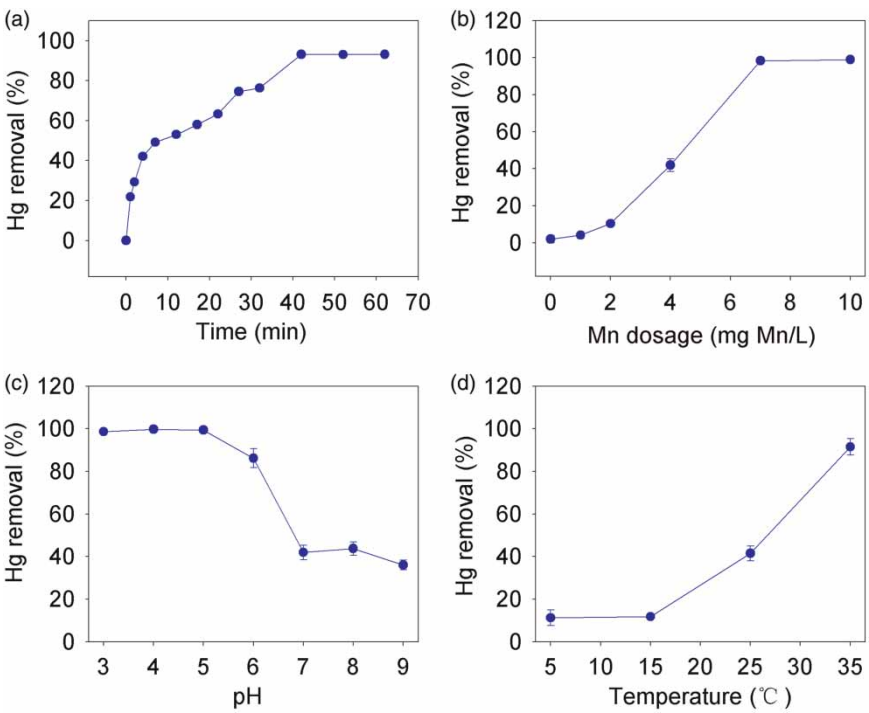

Figure 1 | Hg(II) removal by *in situ* MnO_x adsorption combined with PAC under different experimental conditions. (a) Effect of time; (b) effect of Mn dosage; (c) effect of pH; and (d) effect of temperature.

studies, 'Lemna minor' powder (at 2 g/L) and silica–titania composites (at 1 g/L) were used to decrease mercury concentrations in solution from 20 to 1.9 μg/L and from 100 to 10 μg/L, respectively (Byrne & Mazyck 2009; Li *et al.* 2011). The comparatively low Mn dosages suggest that *in situ* MnO_x may have higher affinity for Hg(II) than both the 'Lemna minor' powder and the silica–titania composites.

Effect of pH

The pH value of the solution was an important factor for mercury removal by *in situ* MnO_x/PAC, as seen in Figure 1(c). At pH lower than 5, the mercury removal was greater than 97% and the residual Hg concentration was less than 1 μg/L. With the increase of pH from 5 to 7, the mercury removal ratio decreased rapidly from 99 to 42%; the ratio of mercury removal remained almost constant for higher pH values. In general, the mercury removal was highly pH-dependent.

A strong dependency of mercury removal on pH was also reported by other researchers (Daughney *et al.* 2002; Herrero *et al.* 2005; Sari & Tuzen 2009; Zabihi *et al.* 2010; Zhang *et al.* 2010) and may have resulted from mercury speciation with the change of pH values. Speciation diagrams calculated with MINEQL+ for Hg(II) in the presence of chloride ions showed more than 98% of the total dissolved mercury as neutral species ($HgCl_2$, Hg(OH)Cl, and $Hg(OH)_2$) in water (Herrero *et al.* 2005; Carro *et al.* 2010). In the present study, the mercury speciation may have been different than that in the presence of chloride ions. There may have been residual $Na_2S_2O_3$ in solution from the *in situ* MnO_x formation process wherein $KMnO_4$ and $Na_2S_2O_3$ were added at a molar ratio of 8/3 for a complete redox reaction to produce MnO_2. The excess $Na_2S_2O_3$ may have reduced *in situ* MnO_x to form Mn^{2+} (Forrez *et al.* 2010) and may also have formed complexes with mercury (Stumm & Morgan 1996; Ma *et al.* 2012). However, the exact species undergoing both the reduction reaction and complexation were not determined for the given experimental conditions. Thus, the molar ratio of $Na_2S_2O_3$/Hg was also analyzed as a function of pH. The mercury species distribution was calculated (Visual MINTEQ 3.0) over the pH range of 0–14 for different molar ratios of $Na_2S_2O_3$/Hg (Figure 2), with a chloride ion concentration of 0.01 mol/L. As the molar ratio of $Na_2S_2O_3$/Hg is increased from 0.5 to 2.0, $Hg(S_2O_3)_2^{2-}$ becomes the main species in the pH range of 3.0–8.0. According to Figure 2, a mercury concentration of 30 μg/L (0.15 μmol/L) would require 0.3 μmol/L $Na_2S_2O_3$

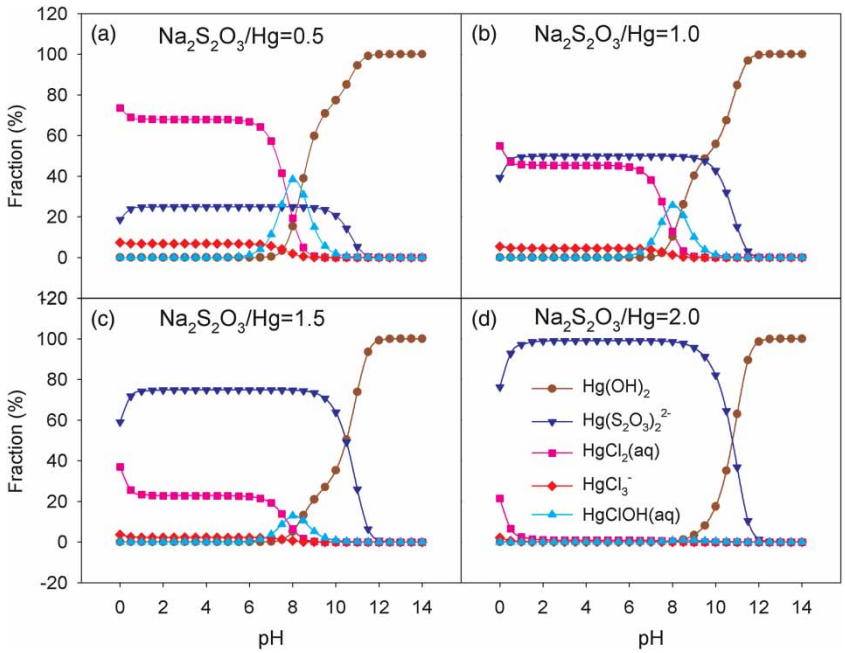

Figure 2 | Mercury species at different $Na_2S_2O_3$/Hg with pH values. Hg concentration, 30 μg/L (0.15 μmol/L); and Cl^-, 0.01 mol/L.

to form $Hg(S_2O_3)_2^{2-}$ complexes at nearly 100%. The required $Na_2S_2O_3$ concentration was ca. 27.3 μmol/L at a molar ratio (8/3) of $KMnO_4$ (5 mg/L for Mn) to $Na_2S_2O_3$ for a complete redox reaction to produce MnO_2. However, the $Na_2S_2O_3$ concentration was ca. 48.5 μmol/L at the molar ratio of 1.5 ($KMnO_4$/$Na_2S_2O_3$) in the present paper. Since the experimental $Na_2S_2O_3$ concentration was greatly in excess of 0.3 μmol/L at approximately 21 μmol/L (48.5–27.3 = 21.2 μmol/L), the main mercury species may have been negatively charged $Hg(S_2O_3)_2^{2-}$, which would be easily adsorbed on the surface of *in situ* MnO_x.

In the process of mercury adsorption on *Aspergillus versicolor* biomass, high adsorption was believed to be a result of a high affinity of the mercury species for certain groups of the biomass (Das *et al.* 2007). Similarly, the high mercury removal at pH lower than 6 may be attributable to the presence of a mercury species ($Hg(S_2O_3)_2^{2-}$) with strong affinity for the active functional groups (–OH) on the surface of *in situ* MnO_x at pH lower than 6, because more Mn ions were produced and may be adsorbed on the surface of *in situ* MnO_x (Forrez *et al.* 2010). The positively charged Mn^{2+} on the surface of MnO_2 can adsorb negatively charged algae (cell or dissolved organic matter (DOM)) (Ma *et al.* 2012), in other words, algae can be indirectly adsorbed on the surface of *in situ* MnO_x by the action of bridge connection (Mn^{2+} as a bridge). Similarly, in the present paper, the Mn^{2+} on the surface of *in situ* MnO_x can act as a cation bridge to enhance mercury adsorption due to mercury species as negatively charged $Hg(S_2O_3)_2^{2-}$. The decrease in ratio of mercury removal with increasing pH may be the result of competitive adsorption between OH^- and $Hg(S_2O_3)_2^{2-}$.

Effect of temperature

Figure 1(d) shows mercury removal ratio as a function of temperature. Mercury removal increased from 11 to ~92% as temperature was increased from 5 to 35 °C. The observed increase of mercury removal ratio with increasing temperature reveals the endothermic nature of mercury removal by *in situ* MnO_x. It also suggests that the available active sites on the surface of *in situ* MnO_x increase with the increasing temperature (Zabihi *et al.* 2010). In addition, the interparticle diffusion of *in situ* MnO_x may be enhanced in an endothermic process, also leading to the increase of mercury removal.

Effect of ionic strength

Ionic strength also had a significant effect on mercury removal, as shown in Figure 3. An increase in the concentration of NaCl from 0.001 to 0.1 mol/L caused a corresponding increase in mercury removal from 18 to 65%. It has been noted that light metal ions such as sodium can compete with heavy metal ions in binding to adsorbents due to electrostatic effects (Schiewer & Wong 2000). However, in this investigation, mercury removal increased as the concentration of light metal ions increased. Therefore, the effect of ionic strength on mercury removal may have been caused by the anions rather than the light metal cations (Herrero *et al.* 2005; Carro *et al.* 2010). Moreover, it is likely that the different anions (e.g. nitrate ions and chloride ions) had different degrees of influence on mercury removal. Nitrate does not form complexes with mercury, as calculated by MINEQL+; hence, mercury removal was not affected by nitrate ions (Carro *et al.* 2010). On the other hand, mercury (Hg(II)) can be complexed with chloride or thiosulfate ions to form neutral mercury species (e.g. $HgCl_2$ and Hg(OH)Cl) and negatively charged species ($HgCl_3^-$, $HgCl_4^{2-}$, and $Hg(S_2O_3)_2^{2-}$). As seen in Figure 2, $Hg(S_2O_3)_2^{2-}$ was likely the dominant species due to excess $Na_2S_2O_3$ in solution. Overall, the calculated mercury species distributions suggest that the mercury removal

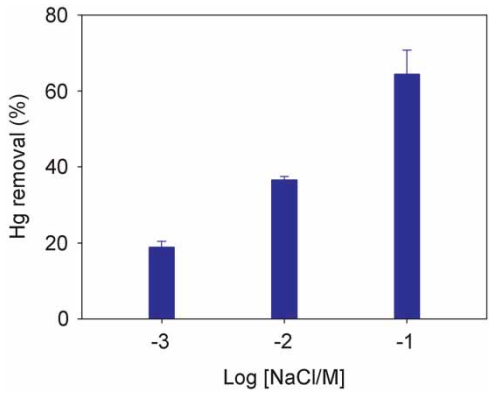

Figure 3 | Hg(II) removal by *in situ* MnO_x adsorption combined with PAC at different ionic strengths. Mn dosage, 4 mg/L; pH, 7.0; time, 15 minutes; and temperature, 25 °C.

ratio increased due to the increase in the proportion of negatively charged mercury species. According to Derjaguin-Landau-Verwey-Overbeek (DLVO) theory and extended DLVO theory (Hermansson 1999; Benítez *et al.* 2007), the *in situ* MnO_x particle and Mn^{2+} formed an electric double layer. The increase in ionic strength (NaCl) from 0.001 to 0.1 mol/L may lead to the thickness of the double layer being compressed, resulting in an increase in the interparticle distance and a decrease in the energy barrier (the point of maximum repulsive energy) between *in situ* MnO_x particles and Mn^{2+} (Hermansson 1999; Benítez *et al.* 2007). Consequently, the Coulomb attractive forces may be enhanced between *in situ* MnO_x particles and Mn^{2+} (Hermansson 1999). According to DLVO theory and extended DLVO theory, the Mn^{2+} on the surface of *in situ* MnO_x particles and $Hg(S_2O_3)_2^{2-}$ may also form an electric double layer (Mn^{2+}–$Hg(S_2O_3)_2^{2-}$). As ionic strength increases, the thickness of the double layer (Mn^{2+}–$Hg(S_2O_3)_2^{2-}$) may be compressed and the energy barrier decreased. As a result, the Coulomb attractive forces may be enhanced between Mn^{2+} and $Hg(S_2O_3)_2^{2-}$. Therefore, the aggregation in MnO_x, Mn^{2+}, and $Hg(S_2O_3)_2^{2-}$ may be enhanced and more easily form aggregate, transferring mercury to the solid phase. This was the reason for the increase in mercury removal.

Based on these results, it may be speculated that the negatively charged mercury species were easily removed by *in situ* MnO_x combined with PAC in the adsorption–flocculation process. Looking ahead, this adsorption–flocculation technology may also be effective for the treatment of water from drinking water sources with higher ionic strengths than were tested for in this investigation.

Removal efficiency

The influence of initial mercury concentration on mercury removal is illustrated in Figure 4. At pH 3 and 5, the mercury removal ratio remained high (with residual mercury concentration at less than 1 μg/L) for initial mercury concentration of up to 30 μg/L (Figure 4(a)). However, at pH 7 and 9, a residual mercury concentration of less than 1 μg/L was only achieved when the initial mercury concentration was less than 10 μg/L. When the initial mercury concentration was more than 30 μg/L (pH 3, 5) and 10 μg/L (pH 7, 9),

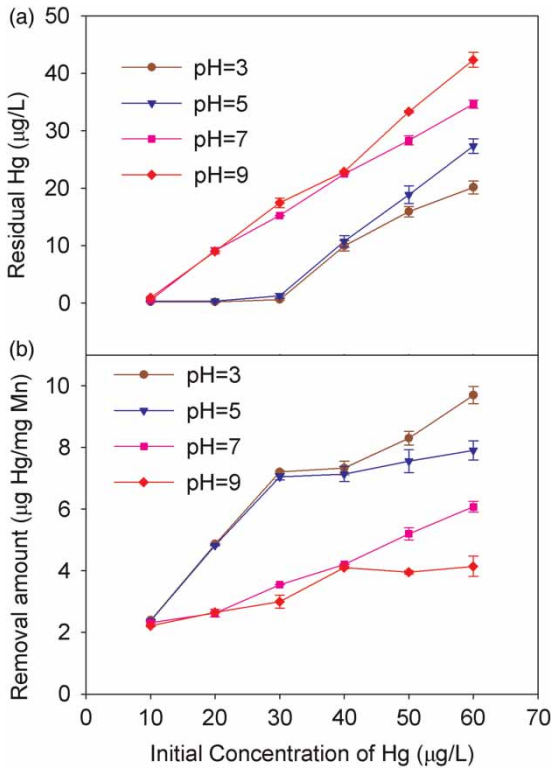

Figure 4 | Hg(II) removal by *in situ* MnO_x adsorption combined with PAC at different initial mercury concentrations. Mn dosage, 4 mg/L; pH, 7.0; time, 15 minutes; and temperature, 25 °C.

the residual mercury concentration increased almost linearly with the increase of mercury concentration. This suggests that *in situ* MnO_x combined with PAC can be effective at removing mercury over a range of different initial mercury concentrations by adjusting the pH value.

The amount of mercury removed (removal amount) is also an important parameter for engineering applications. The removal amount was calculated using the formula as follows:

$$q = \frac{(C_0 - C_r)}{C_{Mn}}$$

where q (μg Hg/mg Mn) is the ratio of the amount of mercury removed to the amount of Mn used, C_0 (μg/L), C_r (μg/L), and C_{Mn} (mg/L) are the initial mercury concentration, the residual mercury concentration, and the *in situ* MnO_x concentration, respectively. Figure 4(b) shows the amount of mercury removed versus the initial mercury concentration at different pH values. In general, the

removal amount increased with the increase of the initial mercury concentration. At pH 3 and 5, the removal amount (q) increased rapidly as the initial mercury concentration was increased up to 30 μg/L. The growth rate of q was retarded at initial mercury concentrations greater than 30 μg/L. A q value of 7.2 μg Hg/mg Mn was observed at the initial mercury concentration of 30 μg/L. By contrast, at pH 7 and 9, q increased slowly as the initial mercury concentration was increased from 10 to 60 μg/L. In this experiment, the maximum q was 9.7 μg Hg/mg Mn at pH 3 when the initial mercury concentration was 60 μg/L.

FTIR and XPS analysis

FTIR spectroscopy was used for the determination of functional groups on the surface of Mn (hydr)oxides, where such information suggests the nature of possible adsorbent metal interactions (Sari & Tuzen 2009; Li *et al.* 2011). The FTIR spectrum of *in situ* Mn (hydr)oxides was obtained and is presented in Figure 5(a). The peak at 1,634 cm^{-1} was caused by the deformation of H–O–H, due to the presence of physisorbed water on the surface of Mn (hydr)oxides. The bands at 1,179 and 979 cm^{-1} were dominated by the bending vibration of the –OH on the surface of Mn (hydr)oxides. The peak at 579 cm^{-1} represents stretching vibrations of Mn–O or Mn–OH (Zhou *et al.* 2001). The analysis of the FTIR spectral results reveals that substantial hydroxyls exist on the surface of the Mn (hydr)oxides. The hydroxyls may act as the surface active adsorption sites for the binding of mercury to the surfaces of Mn (hydr)oxides (Zhang *et al.* 2007).

To further detail the mercury removal process, XPS was used to analyze the chemical states of Mn (hydr)oxides. The results of XPS spectra Mn2p and Hg4f are given in Figures 5(b) and 5(c), respectively. The binding energies of 641.7 eV (representing $Mn2p_{3/2}$) and 653.2 eV (representing $Mn2p_{1/2}$) imply that the primary compound type was MnO_2 or MnOOH (Moulder *et al.* 1992; Biesinger *et al.* 2011). The binding energies at 101.2 and 105.0 eV are assigned to $Hg4f_{7/2}$ and $Hg4f_{5/2}$, respectively (Moulder *et al.* 1992; Behra *et al.* 2001). The presence of Hg4f clearly confirms that mercury transferred to a solid phase from a liquid phase. Furthermore, the Mn2p spectrum suggested that

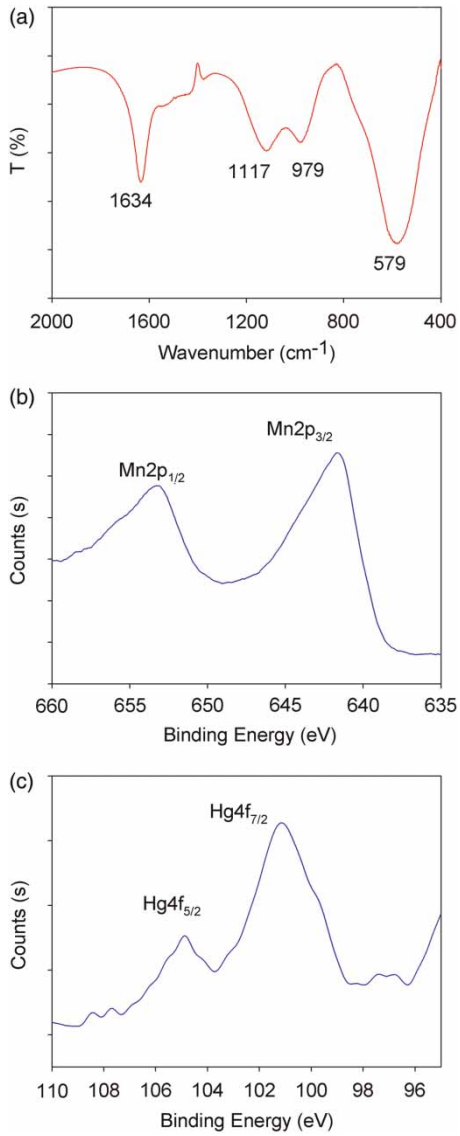

Figure 5 | FTIR and XPS spectra of Hg–Mn mixture. (a) FTIR spectra; (b) XPS spectra of Mn2p core; and (c) XPS spectra of Hg4f core.

MnO_2 or MnOOH played a large role in the adsorption–flocculation process for mercury removal using *in situ* MnO_x combined with PAC.

Based on the above discussion, we conclude that a possible mechanism for trace mercury removal by *in situ* MnO_x combined with PAC is interfacial adsorption with co-precipitation, whereby mercury is transferred to the solid phase from the liquid phase by binding with surface hydroxyls (active adsorption sites), and the subsequent Mn–Hg mixture is precipitated by coagulation using PAC.

Application of *in situ* MnO_x adsorption combined with PAC in water from drinking water source

Trace mercury removal by *in situ* MnO_x combined with PAC was conducted on water from an actual drinking water source and the results are displayed in Figure 6. The initial mercury concentration was set at 30 μg/L by adding mercury to the water. In all experiments, pH values decreased from ca. 7.0 to ca. 5.8. When the Mn dosage was 4 mg/L, mercury removal was greater than 80% and higher than that achieved in the simulated aqueous solution under similar experimental conditions. The difference may be attributable to the large number of suspended solids (SS) in the water, which may have adsorbed mercury. Furthermore, the water contained natural organic matter (NOM), which has abundant functional moieties (e.g. hydroxyl, carboxyl, and phenol groups) that could have adsorbed mercury (Guan *et al.* 2009a; Ma *et al.* 2012). The mercury adsorbed onto SS and NOM could then have been transferred to the precipitate during coagulation. This means that, in the presence of SS and NOM, mercury might be removed even without Mn addition. So we designed experiments whereby mercury was removed by PAC alone to compare with *in situ* MnO_x. However, the mercury removal was ca. 70% when the PAC dosage was from 2 to 50 mg/L (data not shown), suggesting that *in situ* MnO_x was still important for mercury removal. For a Mn dosage of 6 mg/L, the residual mercury concentration was less than 1 μg/L and able to meet the standards for drinking water quality (China). The experimental data obtained for water from a drinking water source suggest that *in situ* MnO_x combined with PAC has the potential to be applied in the practical engineering of trace mercury removal for drinking water treatment.

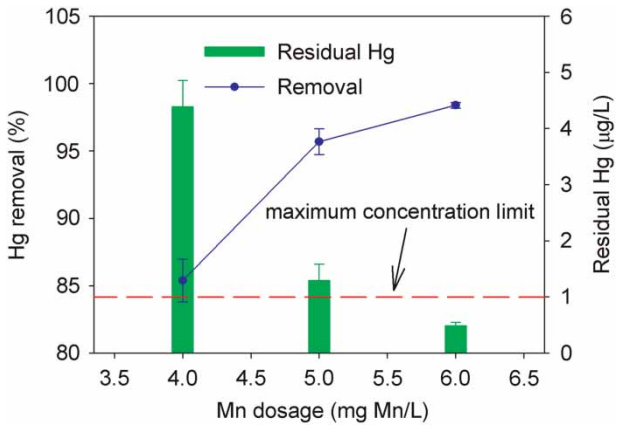

Figure 6 | Hg(II) removal by *in situ* MnO_x adsorption combined with PAC in actual drinking source water. Time, 15 minutes; and temperature, 24 °C.

The residual Mn concentrations after coagulation were measured. However, all Mn concentrations were less than 0.1 mg/L and met the requirements of WHO and China.

CONCLUSIONS

The performance of trace mercury removal by *in situ* MnO_x combined with PAC was affected markedly by the experimental conditions of reaction time, Mn dosage, pH, temperature, and ionic strength. In addition, the amount of mercury removed per amount of Mn added (q) increased with the increase of initial mercury concentration. Based on the FTIR and XPS analyses, the observed high-efficiency mercury removal may be facilitated by the hydroxyl groups (active sites) on the surface of MnO_2 or MnOOH.

The results of the enhanced coagulation experiments using a simulated aqueous solution indicated that *in situ* MnO_x combined with PAC could be used as an effective technology for trace mercury removal. Thus, under the optimized experimental conditions, enhanced coagulation was carried out in water from the drinking water source, and a residual mercury concentration that met the standard for drinking water quality (less than 1 μg/L) was achieved. Consequently, this method offers promising technology for mercury removal from drinking water and other aqueous solutions.

ACKNOWLEDGMENTS

This work was financially supported by the National Science & Technology Pillar Program, China (No. 2012BAC05B02); the Funds for Creative Research Group of China (51121062); the National Natural Science Foundation of China (51008104); the funds of the State Key Laboratory of Urban Water Resource and Environment (HIT, 2013TS04); and the Fundamental

Research Funds for the Central Universities (HIT. NS-RIF. 201188).

REFERENCES

Anirudhan, T. S., Divya, L. & Ramachandran, M. 2008 Mercury (II) removal from aqueous solutions and wastewaters using a novel cation exchanger derived from coconut coir pith and its recovery. *J. Hazard. Mater.* **157** (2–3), 620–627.

Behra, P., Bonnissel-Gissinger, P., Alnot, M., Revel, R. & Ehrhard, J. J. 2001 XPS and XAS study of the sorption of Hg(II) onto pyrite. *Langmuir* **17**, 3970–3979.

Benítez, E. I., Genovese, D. B. & Lozano, J. E. 2007 Effect of pH and ionic strength on apple juice turbidity: application of the extended DLVO theory. *Food Hydrocoll.* **21** (1), 100–109.

Biesinger, M. C., Payne, B. P., Grosvenor, A. P., Lau, L. W. M., Gerson, A. R. & Smart, R. S. C. 2011 Resolving surface chemical states in XPS analysis of first row transition metals, oxides and hydroxides: Cr, Mn, Fe, Co and Ni. *Appl. Surf. Sci.* **257** (7), 2717–2730.

Blue, L. Y., Van Aelstyn, M. A., Matlock, M. & Atwood, D. A. 2008 Low-level mercury removal from groundwater using a synthetic chelating ligand. *Water Res.* **42** (8–9), 2025–2028.

Brown, J. R., Bancroft, G. M. & Fyfe, W. S. 1979 Mercury removal from water by iron sulfide minerals. An electron spectroscopy for chemical analysis (ESCA) study. *Environ. Sci. Technol.* **13** (9), 1142–1144.

Byrne, H. E. & Mazyck, D. W. 2009 Removal of trace level aqueous mercury by adsorption and photocatalysis on silica–titania composites. *J. Hazard. Mater.* **170** (2–3), 915–919.

Carro, L., Anagnostopoulos, V., Lodeiro, P., Barriada, J. L., Herrero, R. & Sastre de Vicente, M. E. 2010 A dynamic proof of mercury elimination from solution through a combined sorption–reduction process. *Bioresour. Technol.* **101** (23), 8969–8974.

Das, S. K., Das, A. R. & Guha, A. K. 2007 A study on the adsorption mechanism of mercury on *Aspergillus versicolor* biomass. *Environ. Sci. Technol.* **41** (24), 8281–8287.

Daughney, C. J., Siciliano, S. D., Rencz, A. N., Lean, D. & Fortin, D. 2002 Hg(II) adsorption by bacteria: a surface complexation model and its application to shallow acidic lakes and wetlands in Kejimkujik National Park, Nova Scotia, Canada. *Environ. Sci. Technol.* **36** (7), 1546–1553.

Forrez, I., Carballa, M., Verbeken, K., Vanhaecke, L., Ternes, T., Boon, N. & Verstraete, W. 2010 Diclofenac oxidation by biogenic manganese oxides. *Environ. Sci. Technol.* **44** (9), 3449–3454.

Guan, X., Dong, H., Ma, J. & Jiang, L. 2009a Removal of arsenic from water: effects of competing anions on As(III) removal in $KMnO_4$–Fe(II) process. *Water Res.* **43** (15), 3891–3899.

Guan, X., Ma, J., Dong, H. & Jiang, L. 2009b Removal of arsenic from water: effect of calcium ions on As(III) removal in the KMnO(4)–Fe(II) process. *Water Res.* **43** (20), 5119–5128.

Guo, Y., Zhao, X. & Tian, Y. 2011 Research of enhanced coagulation as the pretreatment of membrane process in a reclaimed water plant. In: *2011 International Symposium on Water Resource and Environmental Protection. IEEE*, Piscataway, NJ, USA, pp. 2692–2694.

Hermansson, M. 1999 The DLVO theory in microbial adhesion. *Colloids Surf. B Biointerfaces* **14** (1–4), 105–119.

Herrero, R., Lodeiro, P., Rey-Castro, C., Vilarino, T. & de Vicente, M. E. S. 2005 Removal of inorganic mercury from aqueous solutions by biomass of the marine macroalga *Cystoseira baccata*. *Water Res.* **39** (14), 3199–3210.

Inbaraj, B. S., Wang, J. S., Lu, J. F., Siao, F. Y. & Chen, B. H. 2009 Adsorption of toxic mercury(II) by an extracellular biopolymer poly(gamma-glutamic acid). *Bioresour. Technol.* **100** (1), 200–207.

Jeon, C. & Park, K. H. 2005 Adsorption and desorption characteristics of mercury(II) ions using aminated chitosan bead. *Water Res.* **39** (16), 3938–3944.

Jiang, J. Q. & Graham, N. J. D. 1996 Enhanced coagulation using Al/Fe(III) coagulants: effect of coagulant chemistry on the removal of colour-causing nom. *Environ. Technol.* **17** (9), 937–950.

Jiang, G. B., Shi, J. B. & Feng, X. B. 2006 Mercury pollution in China. An overview of the past and current sources of the toxic metal. *Environ. Sci. Technol.* **40** (12), 3673–3678.

Li, S. X., Zheng, F. Y., Yang, H. & Ni, J. C. 2011 Thorough removal of inorganic and organic mercury from aqueous solutions by adsorption on Lemna minor powder. *J. Hazard. Mater.* **186** (1), 423–429.

Ma, J., Graham, N. & Li, G. 1997 Effect of permanganate preoxidation in enhancing the coagulation of surface waters – laboratory case studies. *J. Water Supply Res. Technol. Aqua* **46**, 1–10.

Ma, M., Liu, R., Liu, H. & Qu, J. 2012 Effect of moderate pre-oxidation on the removal of *Microcystis aeruginosa* by KMnO4–Fe(II) process: significance of the in-situ formed Fe(III). *Water Res.* **46** (1), 73–81.

Moulder, J. F., Stickle, W. F., Sobol, P. E. & Bomben, K. D. 1992 *Handbook of X-ray Photoelectron Spectroscopy*. Perkin-Elmer Corporation Physical Electronics Division, Eden Prairie, MN, USA.

Ratto, M., Chiarle, S. & Rovatti, M. 2000 Mercury removal from water by ion exchange resins adsorption. *Water Res.* **34** (11), 2971–2978.

Sari, A. & Tuzen, M. 2009 Removal of mercury(II) from aqueous solution using moss (*Drepanocladus revolvens*) biomass: equilibrium, thermodynamic and kinetic studies. *J. Hazard. Mater.* **171** (1–3), 500–507.

Schiewer, S. & Wong, M. H. 2000 Ionic strength effects in biosorption of metals by marine algae. *Chemosphere* **41** (1–2), 271–282.

Skyllberg, U. & Drott, A. 2010 Competition between disordered iron sulfide and natural organic matter associated thiols for mercury(II) – an EXAFS study. *Environ. Sci. Technol.* **44** (4), 1254–1259.

Song, S., Lopez-Valdivieso, A., Hernandez-Campos, D. J., Peng, C., Monroy-Fernandez, M. G. & Razo-Soto, I. 2006 Arsenic removal from high-arsenic water by enhanced coagulation with ferric ions and coarse calcite. *Water Res.* **40** (2), 364–372.

Stumm, W. & Morgan, J. J. 1996 *Aquatic Chemistry*. John Wiley & Sons, Inc., New York, NY.

Sumesh, E., Bootharaju, M. S. & Anshup, P. T. 2011 A practical silver nanoparticle-based adsorbent for the removal of Hg^{2+} from water. *J. Hazard. Mater.* **189** (1–2), 450–457.

Wagner-Dobler, I., von Canstein, H., Li, Y., Timmis, K. N. & Deckwer, W. D. 2000 Removal of mercury from chemical wastewater by microoganisms in technical scale. *Environ. Sci. Technol.* **34** (21), 4628–4634.

Weisener, C. G., Sale, K. S., Smyth, D. J. A. & Blowes, D. W. 2005 Field column study using zerovalent iron for mercury removal from contaminated groundwater. *Environ. Sci. Technol.* **39** (16), 6306–6312.

Wu, C.-D., Xu, X.-J., Liang, J.-L., Wang, Q., Dong, Q. & Liang, W.-L. 2011 Enhanced coagulation for treating slightly polluted algae-containing surface water combining polyaluminum chloride (PAC) with diatomite. *Desalination* **279** (1–3), 140–145.

Xu, F., Zhang, N., Long, Y., Si, Y., Liu, Y., Mi, X., Wang, X., Xing, F., You, X. & Gao, J. 2011 Porous CS monoliths and their adsorption ability for heavy metal ions. *J. Hazard. Mater.* **188** (1–3), 148–155.

Yan, M., Wang, D., You, S., Qu, J. & Tang, H. 2006 Enhanced coagulation in a typical North-China water treatment plant. *Water Res.* **40** (19), 3621–3627.

Yan, M., Wang, D., Yu, J., Ni, J., Edwards, M. & Qu, H. 2008 Enhanced coagulation with polyaluminum chlorides: role of pH/alkalinity and speciation. *Chemosphere* **71** (9), 1665–1673.

Zabihi, M., Haghighi Asl, A. & Ahmadpour, A. 2010 Studies on adsorption of mercury from aqueous solution on activated carbons prepared from walnut shell. *J. Hazard. Mater.* **174** (1–3), 251–256.

Zhang, G., Qu, J., Liu, H., Liu, R. & Wu, R. 2007 Preparation and evaluation of a novel Fe–Mn binary oxide adsorbent for effective arsenite removal. *Water Res.* **41** (9), 1921–1928.

Zhang, L., Ma, J. & Yu, M. 2008 The microtopography of manganese dioxide formed in situ and its adsorptive properties for organic micropollutants. *Solid State Sci.* **10** (2), 148–153.

Zhang, Y., Li, Q., Sun, L., Tang, R. & Zhai, J. 2010 High efficient removal of mercury from aqueous solution by polyaniline/humic acid nanocomposite. *J. Hazard. Mater.* **175** (1–3), 404–409.

Zhou, M. F., Zhang, L. N., Shao, L. M., Wang, W. N., Fan, K. N. & Qin, Q. Z. 2001 Reactions of Mn with H_2O and MnO with H_2. Matrix-isolation FTIR and quantum chemical studies. *J. Phys. Chem. A* **105** (24), 5801–5807.

Zhou, Y., Xing, X., Liu, Z., Cui, L., Yu, A., Feng, Q. & Yang, H. 2008 Enhanced coagulation of ferric chloride aided by tannic acid for phosphorus removal from wastewater. *Chemosphere* **72** (2), 290–298.

First received 24 June 2014; accepted in revised form 29 September 2014. Available online 27 October 2014